The Journal of Experimental Biology 208, 2023-2036
Published by The Company of Biologists 2005
doi:10.1242/jeb.01611

Functional classification of mitochondrion-rich cells in euryhaline Mozambique tilapia (*Oreochromis mossambicus*) embryos, by means of triple immunofluorescence staining for Na^+/K^+-ATPase, $Na^+/K^+/2Cl^-$ cotransporter and CFTR anion channel

Junya Hiroi[1,*], Stephen D. McCormick[2,3], Ritsuko Ohtani-Kaneko[1] and Toyoji Kaneko[4]

[1]*Department of Anatomy, St Marianna University School of Medicine, Miyamae-ku, Kawasaki 216-8511, Japan,* [2]*USGS, Conte Anadromous Fish Research Center, Turners Falls, MA 01376, USA,* [3]*Department of Biology, University of Massachusetts, Amherst, MA 01003, USA* and [4]*Department of Aquatic Bioscience, Graduate School of Agricultural and Life Sciences, University of Tokyo, Bunkyo-ku, Tokyo 113-8657, Japan*

*Author for correspondence (e-mail: j-hiroi@marianna-u.ac.jp)

Accepted 16 March 2005

Summary

Mozambique tilapia *Oreochromis mossambicus* embryos were transferred from freshwater to seawater and *vice versa*, and short-term changes in the localization of three major ion transport proteins, Na^+/K^+-ATPase, $Na^+/K^+/2Cl^-$ cotransporter (NKCC) and cystic fibrosis transmembrane conductance regulator (CFTR) were examined within mitochondrion-rich cells (MRCs) in the embryonic yolk-sac membrane. Triple-color immunofluorescence staining allowed us to classify MRCs into four types: type I, showing only basolateral Na^+/K^+-ATPase staining; type II, basolateral Na^+/K^+-ATPase and apical NKCC; type III, basolateral Na^+/K^+-ATPase and basolateral NKCC; type IV, basolateral Na^+/K^+-ATPase, basolateral NKCC and apical CFTR. In freshwater, type-I, type-II and type-III cells were observed. Following transfer from freshwater to seawater, type-IV cells appeared at 12 h and showed a remarkable increase in number between 24 h and 48 h, whereas type-III cells disappeared. When transferred from seawater back to freshwater, type-IV cells decreased and disappeared at 48 h, type-III cells increased, and type-II cells, which were not found in seawater, appeared at 12 h and increased in number thereafter. Type-I cells existed consistently irrespective of salinity changes. These results suggest that type I is an immature MRC, type II is a freshwater-type ion absorptive cell, type III is a dormant type-IV cell and/or an ion absorptive cell (with a different mechanism from type II), and type IV is a seawater-type ion secretory cell. The intracellular localization of the three ion transport proteins in type-IV cells is completely consistent with a widely accepted model for ion secretion by MRCs. A new model for ion absorption is proposed based on type-II cells possessing apical NKCC.

Key words: mitochondrion-rich cell, chloride cell, Na^+/K^+-ATPase, $Na^+/K^+/2Cl^-$ cotransporter, cystic fibrosis transmembrane conductance regulator, tilapia, *Oreochromis mossambicus.*

Introduction

In teleost fishes, mitochondrion-rich cells (MRCs, often referred to as chloride cells or ionocytes) in the gill epithelium are the major site of ionic regulation. MRCs are responsible for the secretion of excess ions from the body fluid in seawater-acclimated fish, and possibly in ion uptake in freshwater-acclimated fish (Evans et al., 2005). In embryonic and larval stages without functional gills, MRCs have been detected in the epithelia covering the yolk and body, and these extrabranchial MRCs are considered to be the site of ionic regulation during the early developmental stages (e.g. Hiroi et al., 1998a; Kaneko et al., 2002). In many euryhaline teleost species, both branchial and extrabranchial MRCs are smaller in size and located separately in freshwater, whereas they become larger in size and indented by accessory cells to form multicellular complexes following transfer from freshwater to seawater (Pisam and Rambourg, 1991; Shiraishi et al., 1997).

Recently, by observing *in vivo* sequential changes in individual MRCs in the yolk-sac membrane of Mozambique tilapia *Oreochromis mossambicus* embryos and larvae, we have found that freshwater-type small MRCs possess the ability to survive after direct transfer from freshwater to seawater and to be transformed into seawater-type large MRCs (Hiroi et al., 1999). This implies that MRCs possess the plasticity to alter their ion-transporting functions, from ion absorption to ion secretion. Although our previous study focused on MRC morphology, it is still unclear whether these cells change the direction of ion transport in response to salinity changes.

A currently accepted model for NaCl secretion by MRCs consists of the cooperative action of three major ion transport proteins: Na^+/K^+-ATPase, $Na^+/K^+/2Cl^-$ cotransporter and Cl^- channel (Silva et al., 1977; Marshall, 1995). A Na^+/K^+-ATPase, which is localized to the basolateral membrane of MRCs, creates low intracellular Na^+ and a highly negative charge within the cell. The Na^+ gradient is used to transport Na^+, K^+ and $2Cl^-$ into the cell through a basolateral $Na^+/K^+/2Cl^-$ cotransporter (NKCC). Cl^- then leaves the cells down on an electrical gradient through an apical Cl^- channel, which is homologous to human cystic fibrosis transmembrane conductance regulator (CFTR). Na^+ is transported back outside the cells *via* Na^+/K^+-ATPase, and then secreted by a paracellular pathway between chloride and accessory cells. K^+ is considered to be recycled by a basolateral K^+ channel (Suzuki et al., 1999). This NaCl secretory mechanism by teleost MRCs is comparable to that of mammalian secretory epithelia, such as intestines, airways and salivary glands (Haas and Forbush, 2000).

Recently, basolateral localization of Na^+/K^+-ATPase and NKCC and apical localization of CFTR in MRCs were immunocytochemically demonstrated in seawater-acclimated Hawaiian goby *Stenogobius hawaiiensis*, confirming the current model (McCormick et al., 2003). Therefore, co-localization of all three proteins to MRCs is expected to provide functional evidence that the cells are involved in active ion secretion. In the present study, we transferred Mozambique tilapia embryos directly from freshwater to seawater or from seawater to freshwater, and examined changes in the immunolocalization of Na^+/K^+-ATPase, NKCC and CFTR within MRCs in the yolk-sac membrane using triple-color whole-mount immunofluorescence staining.

Materials and methods

Animals and experimental protocols

Mature Mozambique tilapia (*Oreochromis mossambicus* Peters) were maintained in tanks with recirculating freshwater at 25°C. Fertilized eggs were obtained from the mouth of a brooding female within 1 h after spawning and transferred to hatching jars, in which eggs were agitated gently by aeration. Half the embryos were incubated in freshwater, and the other half were incubated in 32-ppt artificial seawater (Marine Tech, Tokyo, Japan). Water temperature was maintained at 25°C. At this temperature tilapia embryos typically hatch after 5 days in both freshwater and seawater. After 4 day incubation (1 day before hatching), the chorion of embryos was removed with sharp-pointed forceps under a dissecting microscope, and embryos incubated in freshwater were transferred to seawater, and those in seawater were transferred back to freshwater. Each embryo was placed individually in 2 ml of seawater or freshwater in 24-well microplates. The water was renewed daily, and there were no mortalities during the study. Embryos were sampled 0, 12, 24, 48 and 72 h after transfer.

Antibodies

To detect Na^+/K^+-ATPase, a rabbit polyclonal antiserum was directed against a synthetic peptide corresponding to part of the highly conserved region of the Na^+/K^+-ATPase α-subunit (NAK121; Katoh et al., 2000), which was based on the method described by Ura et al. (1996). The specific antibody was purified by affinity chromatography, and conjugated to Alexa Fluor 546 using the Alexa Fluor Protein Labeling Kit (Molecular Probes, Eugene, OR, USA).

The antibody to detect NKCC was mouse monoclonal antibody directed against 310 amino acids at the carboxyl terminus of human colonic NKCC1 (T4, developed by Christian Lytle and Bliss Forbush III, and obtained from the Developmental Studies Hybridoma Bank developed under the auspices of the National Institute of Child Health & Human Development and maintained by The University of Iowa, Department of Biological Sciences, Iowa City, IA, USA). The T4 antibody has been shown to be specifically immunoreactive with NKCC from many vertebrates including teleost fish (Lytle et al., 1995; Wilson et al., 2000a; Pelis et al., 2001; Marshall et al., 2002; McCormick et al., 2003; Wu et al., 2003). The antibody for CFTR was mouse monoclonal antibody against 104 amino acids at the carboxyl terminus of human CFTR (R&D Systems, Boston, MA, USA). To allow triple-color immunofluorescence staining, the mouse monoclonal antibodies against NKCC and CFTR were directly labeled with Alexa Fluor 647 and Alexa Fluor 488, respectively, using the Zenon Mouse IgG Labeling Kits (Molecular Probes). In addition to triple-color direct immunofluorescence staining, conventional single-color indirect immunofluorescence staining with Alexa-conjugated secondary antibodies was carried out for each of the primary antibodies, resulting in the same staining patterns with the triple-color staining. Negative control experiments (without primary antibody) showed no specific staining.

Triple-color whole-mount immunofluorescence staining

The embryos were anesthetized with 2-phenoxyethanol and fixed in 4% paraformaldehyde in 0.1 mol l^{-1} phosphate buffer (pH 7.4) for 90 min at 4°C. The yolk-sac membrane was then incised, the yolk was carefully removed, and the connective tissue and capillaries lining the yolk-sac membrane were removed using sharp-pointed forceps under a dissecting microscope. The membrane was further fixed overnight at 4°C, and preserved in 70% ethanol.

After a rinse with 0.01 mol l^{-1} phosphate-buffered saline containing 0.2% Triton X-100 (PBST, pH 7.2) for 1 h, the fixed yolk-sac membrane was incubated simultaneously with Alexa-Fluor labeled anti-Na^+/K^+-ATPase, anti-NKCC and anti-CFTR for 12 h at 4°C. Anti-Na^+/K^+-ATPase was diluted 1:250. Anti-NKCC and anti-CFTR were used at concentrations of 0.8 μg ml^{-1} and 1.0 μg ml^{-1}, respectively. The antibodies were diluted with PBST containing 0.02% keyhole limpet hemocyanin, 0.1% bovine serum albumin, 10% normal goat serum and 0.01% sodium azide. The membrane was then washed in PBST for 1 h, subjected to post-staining fixation

Table 1. *Classification of four subtypes of mitochondrion-rich cells*

	Type I	Type II	Type III	Type IV
Na^+/K^+-ATPase	Basolateral	Basolateral	Basolateral	Basolateral
NKCC	–	Apical	Basolateral	Basolateral
CFTR	–	–	–	Apical

Mitochondrion-rich cells are defined by immunofluorescence patterns for Na^+/K^+-ATPase, $Na^+/K^+/2Cl^-$ cotransporter (NKCC) and cystic fibrosis transmembrane conductance regulator (CFTR).

with 4% paraformaldehyde for 15 min, washed briefly in PBST, and mounted on a slide with the SlowFade-Light antifade reagent (Molecular Probes).

Both confocal fluorescence and differential interference contrast (DIC) images were taken using a Carl Zeiss 510 META confocal laser scanning microscope with a C-apochromat 40× numerical aperture 1.2, water-immersion objective lens. The wavelengths of excitation and recorded emission for each Alexa dye are as follows: Alexa Fluor 488, 488 nm and 505–530 nm; Alexa Fluor 546, 543 nm and 560–615 nm; and Alexa Fluor 647, 633 nm and 649–756 nm. To avoid any crosstalk, a 'multitrack' configuration was used, in which images were collected successively, rather than simultaneously, on three channels. The size of an optical section was 230 μm × 230 μm × 1 μm (X–Y–Z), and confocal images were taken at 0.5 μm intervals to generate Z-stacks. Ten images corresponding to 0.53 mm^2 were obtained from each sample, while the total surface area of the yolk-sac membrane was approximately 3 mm^2.

Statistics

The cell number and individual cell area of X–Y projection images were measured for four individuals at each sampling time with Photoshop 7.0 (Adobe, San Jose, CA, USA) and the public domain NIH image program (version 1.63, http://rsb.info.nih.gov/nih-image/).

The temporal change in the number of each cell type was analyzed by a one-way analysis of variance (ANOVA; among-groups degrees of freedom=4, within-groups degrees of freedom=15) and the Bonferroni/Dunn *post-hoc* test (Zar, 1999), using Statview 5.0 (SAS Institute, Cary, NC, USA). No significant heterogeneity of variances was detected (Bartlett's test, $P>0.05$). Since the ANOVA and *post-hoc* test were repeated for four cell types, the *P*-value was lowered from the widely used 0.05 to 0.0125 (=0.05/4) to avoid excessive type-I errors.

Results

During the transfer experiments from freshwater to seawater and *vice versa*, four distinct patterns of the immunofluorescence staining for Na^+/K^+-ATPase, NKCC and CFTR were observed within MRCs, and they were defined as type I, type II, type III and type IV (Table 1). The immunoreactivity for the three ion transport proteins in the other cells (e.g. respiratory pavement cells and undifferentiated cells) was negligible. In the following, we first describe staining patterns and general morphological characteristics for those four MRC types, and then address time-course changes in their number and size.

Type-I cell

Type-I cells showed only Na^+/K^+-ATPase immunoreactivity (Fig. 1A,B), while staining for NKCC and CFTR was not detectable (Fig. 1C–F). Strong Na^+/K^+-ATPase immunoreactivity was detectable throughout the cell except for

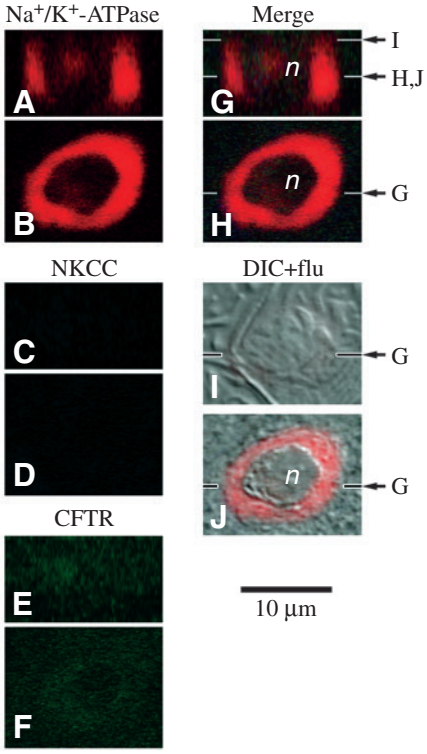

Fig. 1. A typical type-I cell in the yolk-sac membrane of a tilapia embryo at 0 h of the freshwater-to-seawater transfer experiment. (A,C,E,G) X–Z optical sections, cut transversely at the horizontal lines indicated in H, I and J. (B,D,F,H,I,J) X–Y optical sections, cut transversely at the line indicated in G. The immunofluorescence for Na^+/K^+-ATPase, $Na^+/K^+/2Cl^-$ cotransporter (NKCC) and cystic fibrosis transmembrane conductance regulator (CFTR) is shown as separate channels (A–F), and the three channels are merged in G and H. The merged X–Y images are further merged with differential interference contrast images (DIC+flu, I,J). *n*, nucleus. Scale bar, 10 μm.

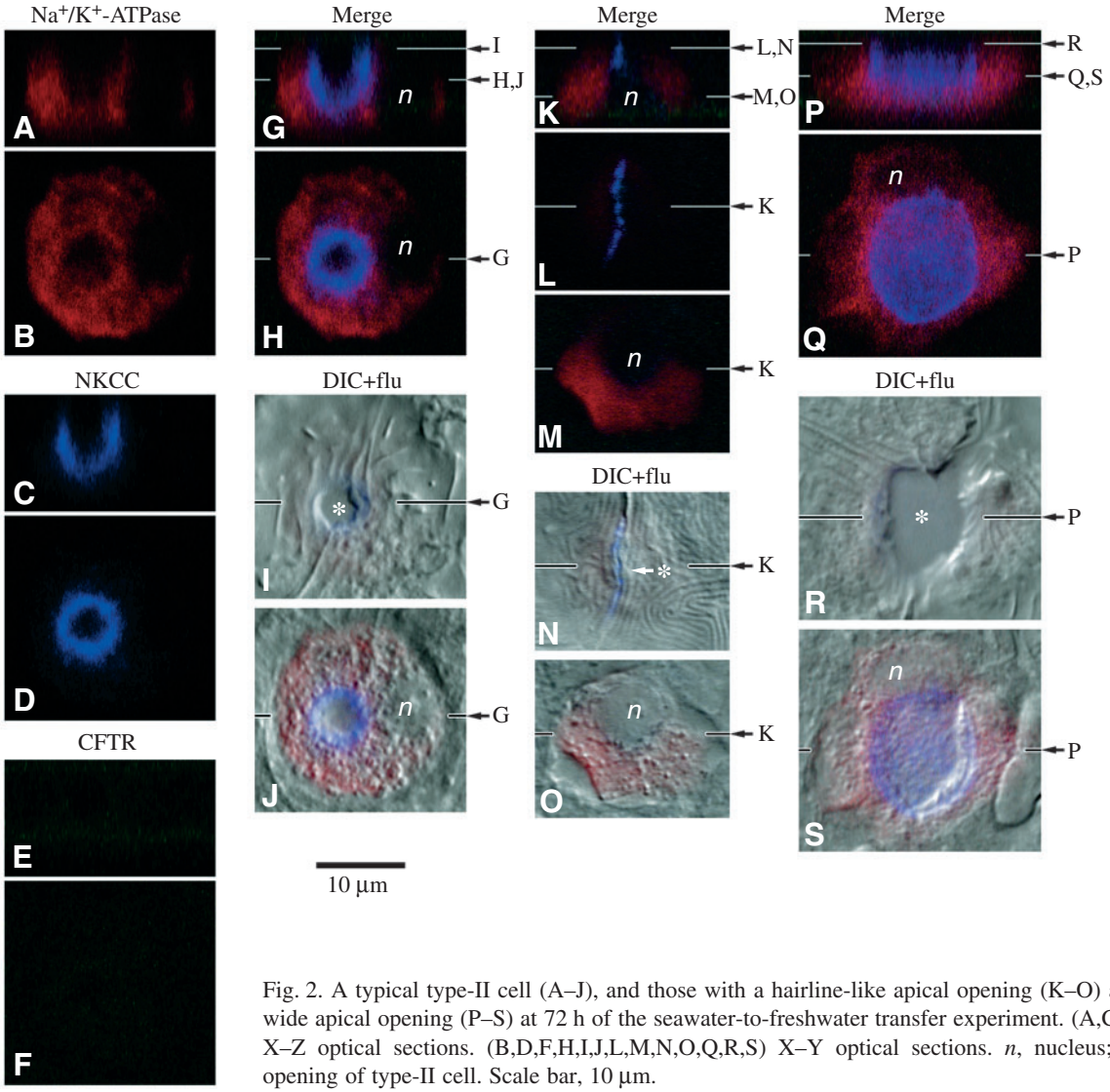

Fig. 2. A typical type-II cell (A–J), and those with a hairline-like apical opening (K–O) and with a wide apical opening (P–S) at 72 h of the seawater-to-freshwater transfer experiment. (A,C,E,G,K,P) X–Z optical sections. (B,D,F,H,I,J,L,M,N,O,Q,R,S) X–Y optical sections. *n*, nucleus; *, apical opening of type-II cell. Scale bar, 10 µm.

the nucleus and sub-apical region (Fig. 1J). When a DIC observation was focused on the surface of the yolk-sac membrane, the ridge structures and boundaries of respiratory pavement cells were observable (Fig. 1I). Underlying MRCs were in focus at a deeper plane (Fig. 1J). The apical opening of the type-I cell was not evident (Fig. 1I), or a pinhole-like apical opening (less than 1 µm in diameter) was found between the boundaries of pavement cells. The type-I cells were relatively small in size and round in shape (occasionally teardrop shape).

Type-II cell

Type-II cells possessed a distinct apical opening at the center of the cell (Fig. 2I), and were characterized by NKCC immunoreactivity at the apical region (Fig. 2C,D). The NKCC staining was concentrated at the apical region and often showed a cup-like appearance (Fig. 2C,D, U-shaped in the X–Z plane and doughnut-shaped in the X–Y plane). The NKCC staining was very weak in the other regions of the cell, not being distinguishable from background levels (Fig. 2C,D). Type-II cells were Na^+/K^+-ATPase positive and CFTR negative, similar to type-I cells (Fig. 2A,B,E,F). Na^+/K^+-ATPase immunoreactivity was detectable throughout the cell except for the nucleus and NKCC-positive apical region (Fig. 2G,H). The Na^+/K^+-ATPase staining was somewhat weaker than that of the type I. The other characteristics of the type II was the same as the type I: smaller in size and round in shape.

Type-III cell

Type-III cells were Na^+/K^+-ATPase positive and CFTR negative, like type I and type II. However, NKCC immunoreactivity was detectable throughout the cell except for the nucleus, coinciding with the staining pattern of Na^+/K^+-ATPase. In Fig. 3G,H, the red color for Na^+/K^+-ATPase and the blue for NKCC were merged into magenta, indicating Na^+/K^+-ATPase and NKCC were co-localized at a pixel level. The type-III cells possessed a distinct apical opening (Fig. 3I), and were mostly larger in size than the types I and II.

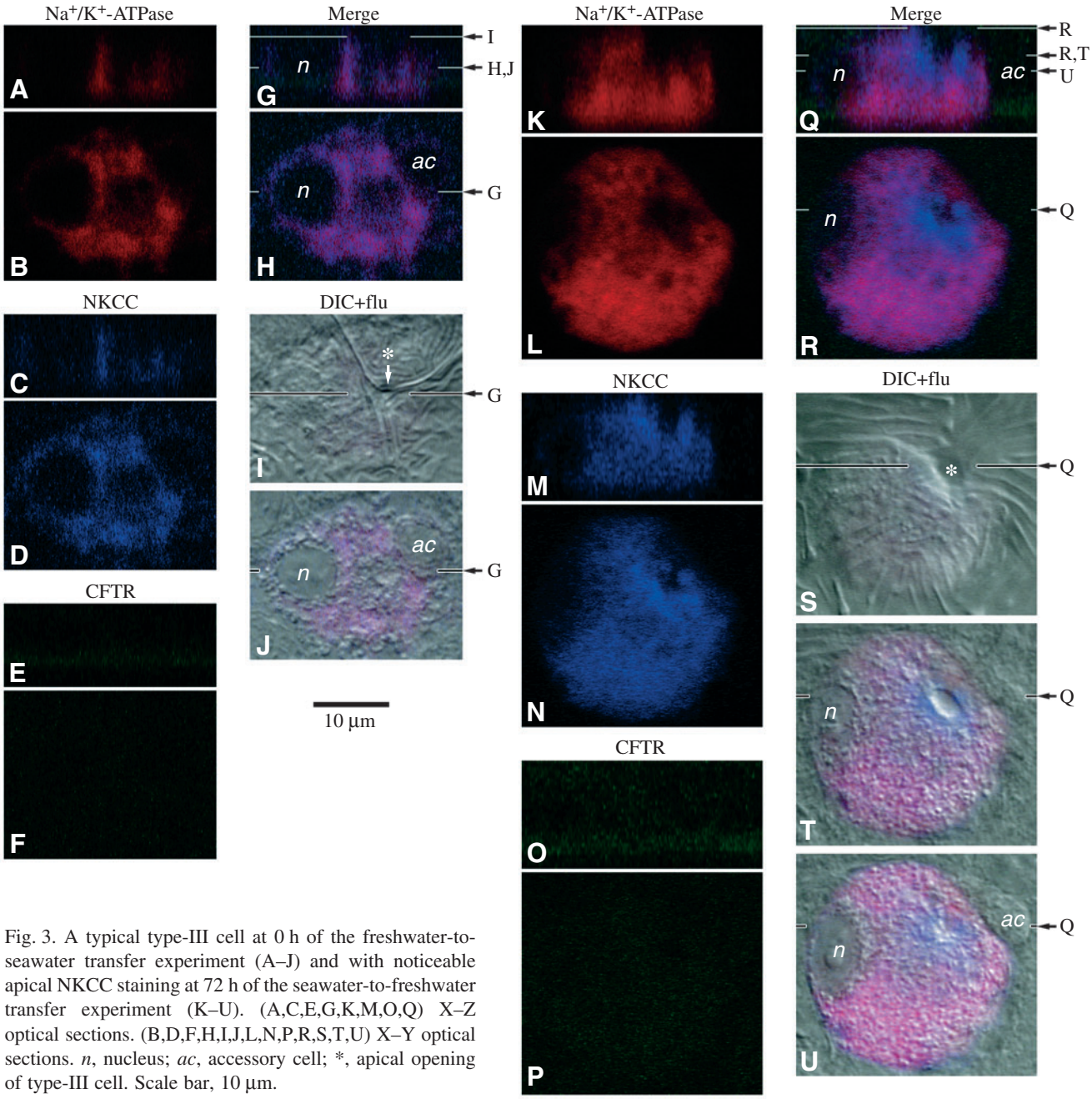

Fig. 3. A typical type-III cell at 0 h of the freshwater-to-seawater transfer experiment (A–J) and with noticeable apical NKCC staining at 72 h of the seawater-to-freshwater transfer experiment (K–U). (A,C,E,G,K,M,O,Q) X–Z optical sections. (B,D,F,H,I,J,L,N,P,R,S,T,U) X–Y optical sections. *n*, nucleus; *ac*, accessory cell; *, apical opening of type-III cell. Scale bar, 10 µm.

Type-IV cell

A prominent feature of the type-IV cell was CFTR immunoreactivity at the apical region. This cell type possessed a large apical crypt (about 5 µm in diameter) at the center of the cell (Fig. 4I,J), and a clear discontinuous, punctate CFTR staining was distributed along the side wall of the crypt (obvious in the X–Y plane, Fig. 4F). The bottom of the crypt and the subapical region showed slight CFTR staining (X–Z plane, Fig. 4E). The immunoreactivity for Na^+/K^+-ATPase and NKCC were detectable throughout the cell except for the nucleus and CFTR-positive apical region (Fig. 4G,H). Occasionally, two or more type-IV cells of similar size joined together and shared a common apical opening (Fig. 4L–O).

Accessory cell

In contrast to type-I cells and type-II cells, type-III cells and type-IV cells were frequently accompanied by one or more small cells that were distinct from pavement cells. Based on its size, location and morphology, this cell type was identified as an accessory cell. The nucleus of the accessory cell was distinguishable by DIC observation, whereas the cytoplasm was indistinct and immunonegative or slightly immunopositive for Na^+/K^+-ATPase (Figs 3J,U and 4J,O). The accessory cells were attached to the edge of type-III cells (Fig. 3J,U), and were located on the shoulder of type-IV cells resulting in a concave appearance of the type-IV cells (Fig. 4G,J,K). Two or more type-IV cells sharing a common

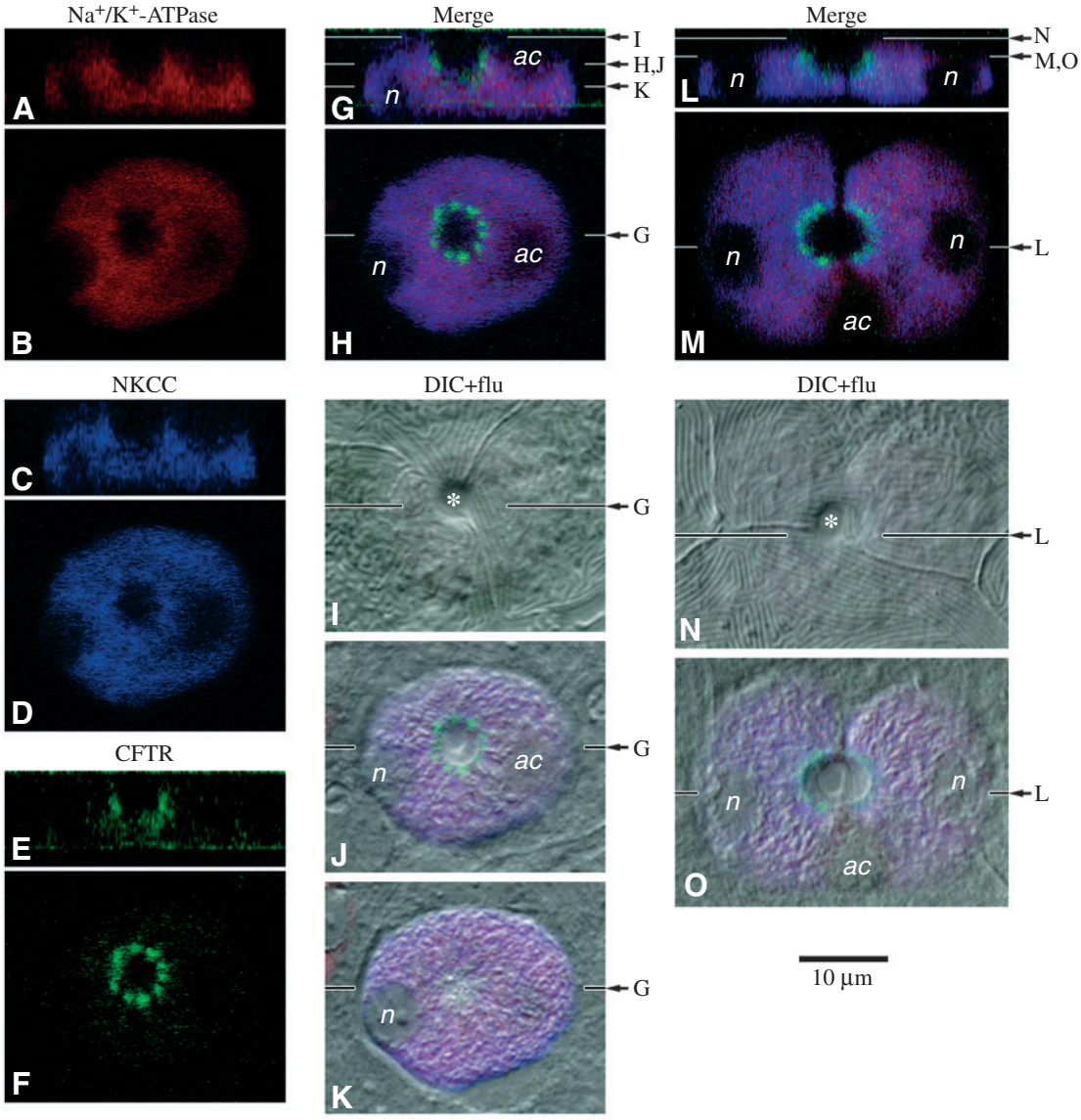

Fig. 4. A typical type-IV cell (A–K) and two type-IV cells of similar size sharing an common apical opening (L–O) at 72 h of the freshwater-to-seawater transfer experiment. (A,C,E,G,L) X–Z optical sections. (B,D,F,H,I,J,K,M,N,O) X–Y optical sections. *n*, nucleus; *ac*, accessory cell; *, apical opening of type-IV cell. Scale bar, 10 µm.

apical opening were also accompanied by accessory cells (Fig. 4O).

Transfer from freshwater to seawater

In embryos kept in freshwater (at 0 h), three types of MRCs without CFTR immunoreactivity, type I, type II and type III, were observed (Fig. 5A–D). Type-IV cells started to appear at 12 h after transfer from freshwater to seawater, and were frequently observed after 24 h. Apical CFTR immunostaining of type-IV cells was not very bright at 12 h and 24 h (Fig. 5G), while bright and punctate CFTR staining was frequently observed at 48 h and 72 h (Fig. 5K). Type-I and type-II cells were observed throughout 72 h of the transfer experiment. Type-III cells decreased in number and disappeared by 72 h.

The ratios of the four types at 0 h were: type I, 30%; type II, 19%; type III, 52%; type IV, 0%. Those at 72 h were: type I, 26%; type II, 6%; type III, 0%; type IV, 68%. The temporal changes in the number of cells (Fig. 6A) were significant for type III (F=44.11, P<0.0001) and type IV (F=22.27, P<0.0001), but were not significant for type I (F=0.45, P=0.77) and type II (F=1.97, P=0.18). The mean number of type-I cells ranged between 129 and 176 cells mm^{-2}, and that of type-II cells decreased from 85 cells mm^{-2} (0 h) to 31 cells mm^{-2} (72 h). The mean number of type-III cells decreased sharply from 279 cells mm^{-2} (12 h) to 29 cells mm^{-2} (24 h), whereas that of type-IV cells increased from 37 cells mm^{-2} (12 h) to 254 cells mm^{-2} (24 h) (P<0.0125 between 0–12 h and 24–72 h for both cell types).

Size/frequency distributions of the cell types existing at 0 h and 72 h (types I, II and III for 0 h; types I, II and IV for 72 h) are shown in Fig. 7A. Size distributions of type-I and type-II cells were narrow, whereas those of type-III and type-IV cells were wider with a greater number of larger cells. The size distributions of type-III cells at 0 h and type-IV cells at 72 h were positively skewed (i.e. there were small numbers of very large cells).

Transfer from seawater to freshwater

In embryos kept in seawater (at 0 h), large type-IV cells were frequently observed, together with relatively smaller numbers of type-I and type-III cells (Fig. 5M–P). Following transfer from seawater to freshwater, apical CFTR staining of type-IV cells faded, the number of type-IV cells decreased at 24 h, and they disappeared at 48 h and 72 h. By contrast, type-III cells increased in number following transfer. Type-II cells were not found at 0 h, but started to appear at 12 h and were frequently observed after 24 h. The apical NKCC staining of type-II cells was a pinhole-like small spot or a short and straight hairline at 12 h and 24 h (Fig. 5R), and became larger at 48 h and 72 h (Fig. 5V). Type-I cells were observed throughout the transfer experiment.

The ratios of the four cell types at 0 h were: type I, 14%; type II, 0%; type III, 13%; type IV, 73%. Those at 72 h were: type I, 15%; type II, 25%; type III, 60%; type IV, 0. The temporal changes in the number of cells (Fig. 6B) were significant for type II (F=6.73, P=0.0026), type III (F=23.34, P<0.0001) and type IV (F=75.61, P<0.0001), but were not significant for type I (F=0.62, P=0.65). The mean number of type-I cells ranged between 52 and 75 cells mm^{-2}. Type-II cells were not found at 0 h, first appeared at 12 h (14 cells mm^{-2}), and reached 99 cells mm^{-2} at 72 h (P<0.0125 between 0 h and 48–72 h). From 0–12 h to 24–72 h, the mean number of type-III cells increased sharply from 77 cells mm^{-2} (12 h) to 285 cells mm^{-2} (24 h), whereas that of type-IV cells decreased from 240 cells mm^{-2} (12 h) to 31 cells mm^{-2} (24 h) (P<0.0125 between 0–12 h and 24–72 h for both cell types).

Size/frequency distributions of the cell types existing at 0 h and 72 h (type I, type III and type IV for 0 h; type I, type II and type III for 72 h) are shown in Fig. 7B. The size distributions of type-I and type-II cells were narrower than for type-III and type-IV cells which had distinctive bimodal distributions (peak: 200–250 μm^2 and 450–500 μm^2 for type III+type IV at 0 h; 200–250 μm^2 and 500–550 μm^2 for type III at 72 h).

Discussion

MRCs of euryhaline teleosts have been considered to be responsible for two opposite vectorial ion movements: ion secretion in seawater and ion absorption in freshwater. The localization of patterns of ion transport proteins on the apical and basolateral membrane of MRCs are important for determining the transport functions of these cells. In the present study, we applied simultaneous immunofluorescence staining for Na^+/K^+-ATPase, NKCC and CFTR to MRCs of tilapia embryos. This is the first study to ascertain the intracellular localization of the three major ion transport proteins at a single cell level, not only in teleost MRCs but also in ion transport epithelial cells in general. We were able to classify MRCs into four types, types I, II, III and IV. Taking account of the localization patterns of the three proteins and changes in cell numbers of the four types in response to salinity changes (as well as previous studies on the functional attributes of MRCs), we deduce that type I is an immature MRC, type II is a freshwater-type ion absorptive cell, type III is a proto- or dormant-type of type IV, and type IV is a seawater-type ion secretory cell. In the following, we will discuss each cell type in detail.

Seawater-type ion secretory cell

Type-IV cells were the only type showing immunoreactivity for all three ion transport proteins examined, Na^+/K^+-ATPase, NKCC and CFTR (Fig. 4). The intracellular distributions of both Na^+/K^+-ATPase and NKCC were throughout the cell except for the nucleus and the apical region. Previous electron microscopic studies have demonstrated that Na^+/K^+-ATPase was present on both the basolateral membrane and the extensive tubular system, which was continuous with the basolateral membrane of MRCs (Evans et al., 2005). Therefore, the presence of Na^+/K^+-ATPase and NKCC within MRCs represents their basolateral distributions. The basolateral distributions of Na^+/K^+-ATPase and NKCC and a distinct apical CFTR distribution in type-IV cells are completely consistent with the current accepted model for ion secretion by MRCs, indicating that type-IV cells are seawater-type ion secretory cells. This is also supported by our finding that type-IV cells were purely seawater specific: they were not observable in freshwater, rapidly appeared following transfer from freshwater to seawater (Fig. 6A), and disappeared following transfer from seawater to freshwater (Fig. 6B).

Type-III cells showed basolateral staining of Na^+/K^+-ATPase and NKCC, but lacked apical CFTR staining. Following transfer from freshwater to seawater, the number of type-III cells decreased whereas type-IV cells increased, and the size/frequency distribution of type-III cells at 0 h and that of type IV cells at 72 h showed similar unimodal, positively skewed distributions. Based on these observations, we propose that after seawater exposure type-III cells synthesize CFTR *de novo* and arrange it at the apical membrane following transfer from freshwater to seawater, and consequently the cells are counted as type-IV cells. Transfer from seawater to freshwater showed these changes in reverse: the numbers of type-III cells increased whereas type-IV cells decreased, and the size of type III+type IV at 0 h and that of type III at 72 h had similar bimodal distributions. Therefore, it is most likely that type-IV cells lose apical CFTR and stop their ion secretory function to change into type-III cells following transfer from seawater to freshwater. From these observations, we conclude that type-III cells are a proto- or dormant-type of type-IV cells that only becomes active in ion secretion after placement of CFTR in the apical membrane.

Our previous *in vivo* sequential observations revealed that 75% of pre-existing MRCs in tilapia embryos survived for 96 h following transfer from freshwater to seawater (Hiroi et al., 1999). After transfer from freshwater to seawater in the present study, the number of type-III cells at 0 h and that of type-IV cells at 72 h corresponded to 50% (233 cells mm^{-2}) and 75% (345 cells mm^{-2}) of total pre-existing cells at 0 h of freshwater-to-seawater transfer (452 cells mm^{-2}), respectively (stacked

graph in Fig. 6A). Therefore, almost all type-III cells are expected to survive to be transformed into type-IV cells, while the remaining type-IV cells would be differentiated from type-I cells (presumptive immature MRCs; see below). The *in vivo* sequential observations also demonstrated that each surviving cell enlarged following seawater transfer, similar to the present results in which the size of type-IV cells at 72 h exceeded that of type-III cells at 0 h (Fig. 7A). Therefore, the transformation from type III to type IV would include not only the appearance of apical CFTR but also the increase in cell size, which may imply the enlargement of the basolateral/tubular system in order to localize more Na^+/K^+-ATPase and NKCC for active NaCl secretion in seawater.

The transition between types III and IV reflects the appearance and disappearance of apical CFTR immunoreactivity in MRCs, and these changes started within 12 h and occurred sharply between 12 h and 24 h after transfer from freshwater to seawater and *vice versa* (Fig. 6). The similar rapid CFTR response to salinity change was observed in killifish *Fundulus heteroclitus*: following transfer from freshwater to seawater, CFTR mRNA started to increase at 8 h and showed a ninefold increase at 24 h (Singer et al., 1998),

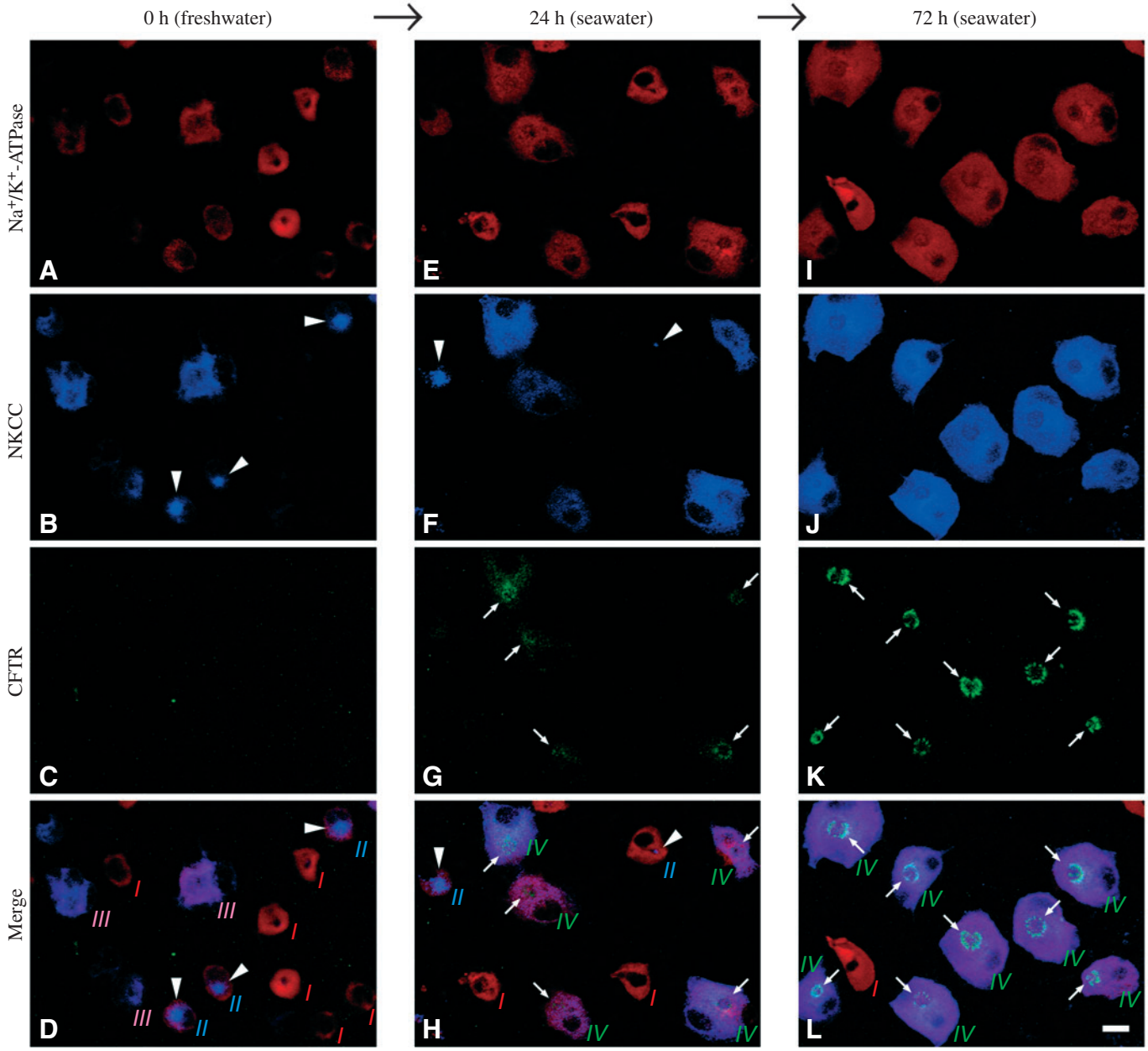

Fig. 5. X–Y projection images of immunofluorescence staining for Na^+/K^+-ATPase, $Na^+/K^+/2Cl^-$ cotransporter (NKCC) and cystic fibrosis transmembrane conductance regulator (CFTR), at 0 h (A–D), 24 h (E–H) and 72 h (I–L) of the freshwater-to-seawater transfer experiment, and at 0 h (M–P), 24 h (Q–T) and 72 h (U–X) of the seawater-to-freshwater transfer experiment. Arrowheads and arrows indicate apical NKCC staining and apical CFTR staining, respectively. I, type-I cell; II, type-II cell; III, type-III cell; IV, type-IV cell. Scale bar, 10 μm.

and apical CFTR immunoreactivity in MRCs increased between 24 h and 48 h (Marshall et al., 2002); following transfer from seawater to freshwater, apical CFTR immunoreactivity was reduced at 12 h and disappeared at 24 h (Katoh et al., 2003). Therefore, tilapia and killifish, the two typical experimental models for euryhaline fish, seem to share a similar on–off mechanism of active ion secretion, which is achieved by the rapid appearance and disappearance of CFTR at the apical membrane of MRCs. It has also been reported that MRCs close the apical openings quickly (about 30 min or a few hours, which seem likely to be quicker than the response of CFTR) in response to abrupt salinity changes or acid–base disturbances (Goss et al., 1995; Sakamoto et al., 2000; Daborn et al., 2001; Lin and Hwang, 2004). Although we confirmed in DIC observations that all of the type-III cells that appeared following transfer from seawater to freshwater possessed a distinct apical opening, it is possible that the apical opening of the MRCs was closed within 12 h, in advance of the disappearance of the apical CFTR distribution.

The noticeable characteristics of type-IV cells were clear discontinuous, punctate CFTR staining at the apical region (Fig. 4F,H,M) and indentation by accessory cells (Fig. 4G,H,J,M,O). A similar punctate distribution of apical CFTR was observed in seawater-adapted Hawaiian goby (McCormick et al., 2003). Shiraishi et al. (1997) presented transmission electron micrographs of a horizontal section cut through an apical crypt of a seawater-type MRC in the yolk-sac membrane of the same species. In the micrographs, an accessory cell interdigitated with a main MRC, and extended cytoplasmic processes to the apex, so that cytoplasmic

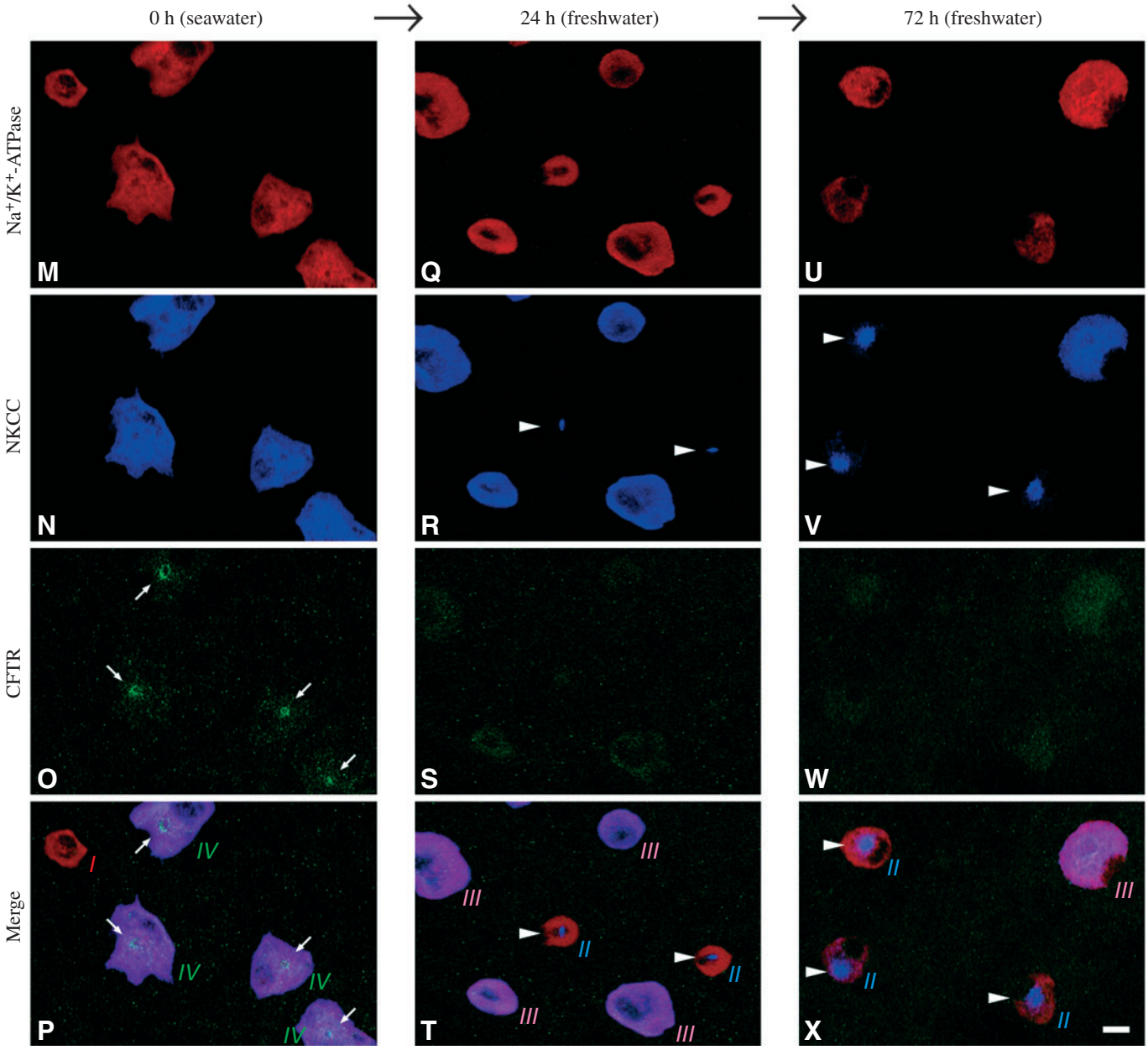

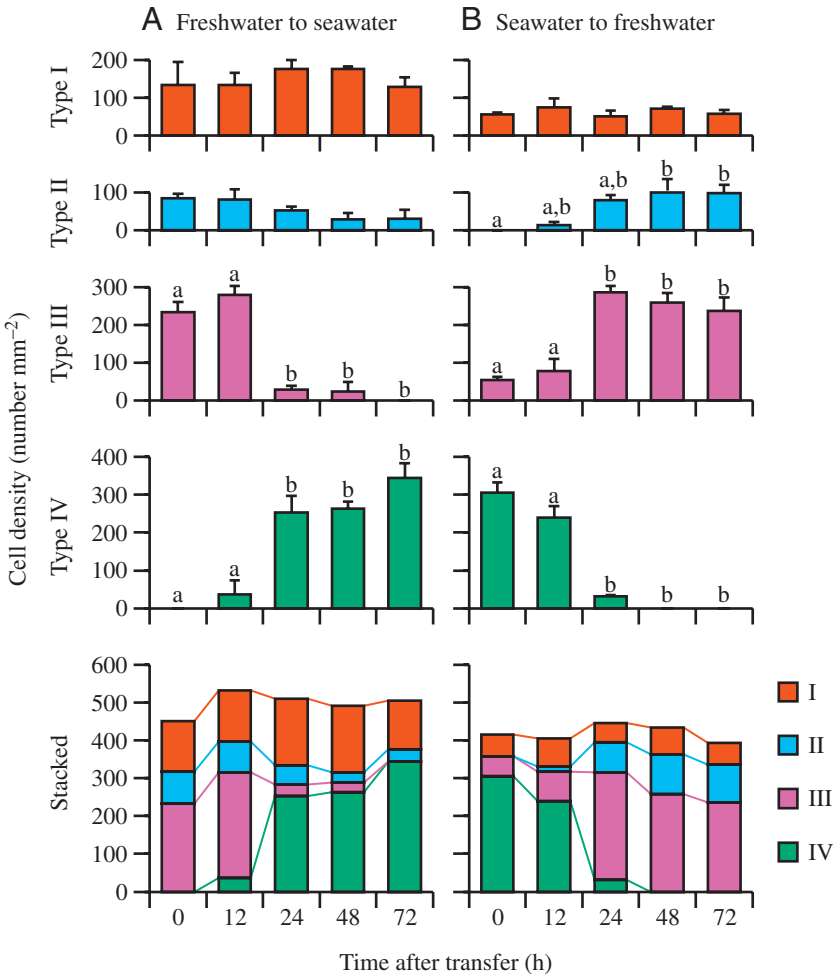

Fig. 6. Changes in the density of the four mitochondrion-rich cell types following transfer from freshwater to seawater (A) and *vice versa* (B). The data are expressed as the mean ±S.E.M. of four individuals. Columns with different letters are significantly different (P<0.0125, the Bonferroni/Dunn test). red, type-I cell; cyan, type-II cell; magenta, type-III cell; green, type-IV cell.

processes of the MRCs and accessory cells appeared to be arranged alternately. Supposing that CFTR is present only in the MRC itself and not in the interdigitating accessory cell, the apical CFTR staining may result in a discontinuous pattern associated with the alternate arrangement of the interdigitation. Thus, the discontinuous CFTR staining in the present study would reflect the complex architecture between chloride and accessory cells. In the current model for NaCl secretion by MRCs, while Cl^- is considered to be secreted through MRCs, Na^+ secretion occurs *via* a paracellular pathway formed between chloride and accessory cells. Therefore, the discontinuous CFTR staining might indirectly imply type-IV cells as the site not only for Cl^- secretion but also that they are involved in paracellular Na^+ secretion. Previous transmission electron microscopic studies revealed that the interdigitation and leaky junction between chloride and accessory cells appeared within 1–3 h after transfer of larval Ayu *Plecoglossus altivelis* from freshwater to seawater, and disappeared within 3 h after transfer of juvenile stone flounder *Kareius bicoloratus* from seawater to freshwater (Hwang and Hirano, 1985; Hwang, 1990). We consider it likely that the development and degeneration of the interdigitation between chloride and accessory cells occurs reversibly in parallel with the appearance and disappearance of CFTR at the apical membrane of MRCs.

Freshwater-type ion absorptive cell

Type-II cells possessed apical NKCC, basolateral Na^+/K^+-ATPase and showed freshwater-specific changes in number during the transfer experiments: type-II cells were absent in seawater, appeared following transfer from seawater to freshwater (Fig. 6B), and tended to decrease following transfer from freshwater to seawater (Fig. 6A). These changes in response to salinity changes provide indirect evidence that type-II cells possess an ion transport function favorable for freshwater acclimation, presumably ion absorption.

The apical localization of NKCC in MRCs is surprising. A number of previous reviews on ion transport mechanisms of teleost gills have suggested Na^+ absorption by H^+-ATPase and Na^+ channel, or by a Na^+/H^+-exchanger, and Cl^- absorption by Cl^-/HCO_3^- exchanger, but did not refer to apical NKCC (e.g. Marshall, 2002; Perry et al., 2003; Evans et al., 2005). An active NaCl uptake mechanism with apical NKCC has been proposed in crabs *Carcinus maenas* and *Chasmagnathus granulatus* in brackish water (Riestenpatt et al., 1996; Onken et al., 2003), and only Kirschner (2004) has proposed that the mechanism may exist in estuarine fish. In other euryhaline teleost species examined so far, the presence of apical NKCC has not been reported: in Atlantic salmon *Salmo salar* and Hawaiian goby, NKCC has a basolateral localization in MRCs in both freshwater and seawater conditions (Pelis et al., 2001; McCormick et al., 2003); in killifish, NKCC is condensed and localized in lateral parts of MRC complexes in freshwater, and apparently not in the apical membrane area of MRCs (Marshall et al., 2002). Apical NKCC staining is currently detectable only in MRCs in the gills (Wu et al., 2003) and in the embryonic yolk-sac membrane (present study) of freshwater-acclimated Mozambique tilapia.

In mammals, the $Na^+/K^+/2Cl^-$ cotransporter occurs in two major isoforms: a secretory isoform, termed NKCC1, and an absorptive isoform, termed NKCC2 (Xu et al., 1994; Payne and Forbush, 1994). NKCC1 is widely distributed in mammalian tissues and is especially prominent in secretory epithelial cells, in which NaCl is secreted in the same manner as seawater-type MRCs. By contrast, NKCC2 is found only in the apical

membrane of epithelial cells in the thick ascending limb of the loop of Henle (TAL) (Lytle et al., 1995; Kaplan et al., 1996; Nielsen et al., 1998). The localization and stoichiometry of the NKCC2 appears to be conserved among vertebrates, though alternative splicing results in altered affinities (Gagnon et al., 2003). In the TAL, NKCC and K^+ channel (ROMK, Xu et al., 1997) are present at the apical membrane, whereas Na^+/K^+-ATPase and Cl^- channel (CLC-K2, Uchida, 2000) are in the basolateral membrane. In the present study, the presence of two out of four proteins, apical NKCC and basolateral Na^+/K^+-ATPase defined type-II cells. Therefore, it is possible that type-II cells are involved in NaCl absorption by the same manner as mammalian TAL epithelial cells. It should be noted, that the luminal Na^+ concentration in the TAL is higher than the intracellular Na^+, providing a driving force for the NKCC to transport Na^+, K^+ and $2Cl^-$ into the cell, whereas this would be absent under most freshwater conditions (Na^+ concentrations of freshwater are lower than the Na^+ concentration in MRCs). It is possible that this uptake mechanism may only function when ambient Na^+ is relatively high (e.g. >10 mmol l^{-1}), or that intracellular Na^+ near the apical membrane is kept at very low levels in these cells by basolateral Na^+/K^+-ATPase. If the type-II cell is indeed involved in uptake, it seems likely that the observed apical staining is an NKCC2-like absorptive isoform, since the anti-NKCC (T4) used in this study is known to react with both NKCC isoforms (Lytle et al., 1995). We have recently succeeded in isolating two homologs of NKCC1 (GenBank accession No. AY513737, AY513738) and one homolog of NKCC2 (AY513739) from the gills of adult Mozambique tilapia. Ascertaining the cellular distribution of these NKCC genes and the immunolocalization of their proteins will help clarify their involvement in ion absorption and secretory processes.

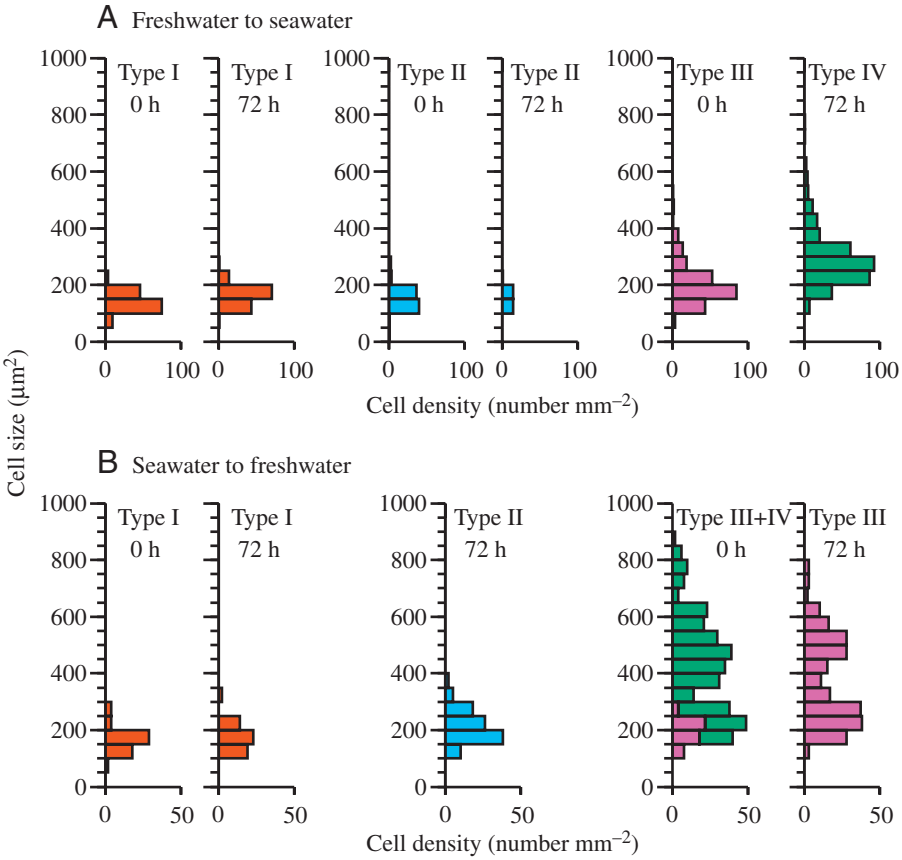

Fig. 7. Size/frequency distributions of the mitochondrion-rich cell types existing at 0 h and 72 h of the freshwater-to-seawater transfer experiment (A) and seawater-to-freshwater transfer experiment (B). Data of four individuals were pooled for each histogram. red, type-I cell; cyan, type-II cell; magenta, type-III cell; green, type-IV cell.

The apical NKCC staining of type-II cells showed some variations during the transfer experiments. Type-II cells with a cup-like apical NKCC staining (Fig. 2A–J) were frequently observed in embryos fully acclimated to freshwater, at 0 h of freshwater-to-seawater transfer and at 48 and 72 h of seawater-to-freshwater transfer. On the other hand, type-II cells with pinhole-like or hairline-like apical NKCC staining, which corresponded with the boundaries between pavement cells (Fig. 2K–O), appeared at 12 h and 24 h of seawater-to-freshwater transfer. These cells seem to be an earlier developmental stage of type-II cells that have just differentiated from type-I cells, and are expected to enlarge the apical opening and place more NKCC at the apical membrane during freshwater acclimation.

Previous morphological observations on the same species identified three types of MRCs with different apical surfaces: wavy convex, shallow basin and deep hole (Lee et al., 1996; Lin and Hwang, 2001, 2004). The wavy-convex-type cells, which possessed a wide apical opening and a rough apical surface appearance, increased in number in low Cl^- water, suggesting this cell type is involved in active Cl^- uptake. We also recognized a small number of type-II cells (approximately less than 5%) possessed a wide apical opening and a rough apical surface appearance 72 h after transfer from seawater to freshwater (Fig. 2P–S). Although the apical surface of the cells looked concave, not convex, this may have been due to the removal of the yolk-sac membrane in the present study, which may change a convex apical surface into a concave one. Therefore, these type-II cells seem likely to be identical to the wavy-convex-type cells, and it is of great interest to determine whether they proliferate in low Cl^- conditions.

Although type-III cells are unlikely to be involved in ion secretion, the possibility that they are involved in ion absorption in freshwater condition cannot completely ruled out. Wilson et al. (2000b) reported that H^+-ATPase and Na^+

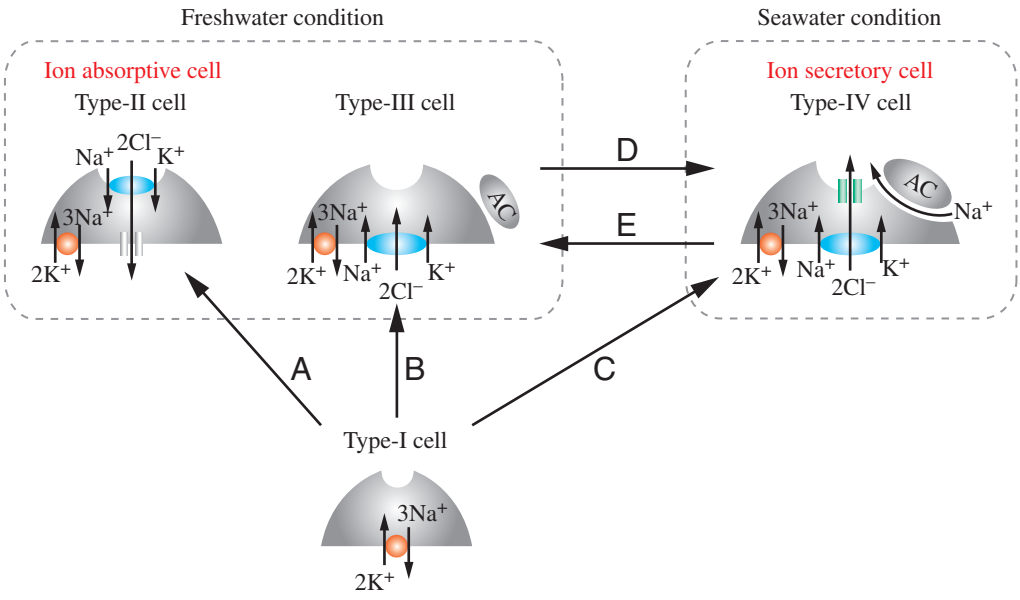

Fig. 8. Schematic diagrams of the four mitochondrion-rich cell types, showing intracellular localization of Na^+/K^+-ATPase (red), $Na^+/K^+/2Cl^-$ cotransporter (NKCC, cyan) and cystic fibrosis transmembrane conductance regulator (CFTR, green). The movements of ions are focused on Na^+ and Cl^-, and a K^+ channel recycling K^+ is omitted in order to simplify the diagrams. A Cl^- channel (gray) is added on the basolateral membrane of the type-II cell, although its presence was not examined in this study. The presumed interrelationship among the four cell types are indicated by arrows A–E.

channel immunoreactivity were co-localized to pavement cells, and apical Cl^-/HCO_3^- exchanger immunoreactivity was found in MRCs in the gills of the same species, proposing that the absorption of Na^+ and Cl^- occurs separately in pavement cells and MRCs, respectively. H^+-ATPase immunoreactivity was also found in pavement cells in the yolk-sac membrane of tilapia larvae (Hiroi et al., 1998b). Therefore, if Cl^-/HCO_3^- exchanger is localized in the apical membrane of type-III cells, the cell type could be involved in Cl^- absorption. There is evidence that there are different ion uptake mechanisms in zebrafish (*Danio rerio*) acclimated to soft water and hard water (Boisen et al., 2003), and it is also possible that different ion uptake mechanisms by different cell types exist concurrently and are regulated by ambient ion levels. Future studies on the localization of the $Cl^-/HCO3^-$ exchanger as well as other ion transport proteins in relation to ambient ion changes are warranted. Moreover, some type-III cells appearing after transfer from seawater to freshwater showed relatively strong NKCC staining at the apical region, in which Na^+/K^+-ATPase staining was absent (Fig. 3K–U). We counted these cells as type-III cells rather than type-II cells, because of their distinct basolateral NKCC staining (type-II cells were defined as showing apical NKCC and basolateral Na^+/K^+-ATPase, without basolateral NKCC). These type-III cells might synthesize absorptive type NKCC *de novo*, arrange it at the apical membrane and function as the ion absorptive site in the same manner as type-II cells. The development of antibodies that can distinguish absorptive and secretory isoforms of NKCC is expected to specify the function of these cells further.

Immature MRC

Previous transmission electron microscopic studies revealed the developmental stages of MRCs in the same species: accessory, immature, mature and degenerating cells (Wendelaar Bonga and van der Meij, 1989; van der Heijden et al., 1999). They reported that immature MRCs had less-developed tubular system than in mature cells, and most immature cells did not contact the outside medium. Type-I cells were characterized by their relatively small size, indistinct apical opening and possessing only Na^+/K^+-ATPase immunoreactivity, indicating they are probably immature MRCs. As such, they are expected to develop into other MRC types: types II, III and IV. Type-I cells existed consistently during both transfer experiments, suggesting that the recruitment of new MRCs occurs irrespective of salinity changes. This accords well with previous *in vivo* sequential observations in which the same rate of MRC turnover was observed in both freshwater and seawater (Hiroi et al., 1999).

In conclusion, the characteristics of the four MRC types and their presumptive interrelationships are summarized in Fig. 8. Immature type-I cells are considered to develop into type-II ion absorptive cells (arrow A in Fig. 8) and type-III cells (arrow B) in freshwater, and into type-IV ion secretory cells in seawater (arrow C). Following transfer from freshwater to seawater, it seems likely that most type-III cells are transformed into type-IV cells (arrow D), while a certain number of type-I cells may also develop into type-IV cells (arrow C). When transferred from seawater back to freshwater, type-IV cells seem to change into type-III cells to stop ion secretion (arrow E), and type-I cells develop into type-II cells to function as in ion absorption (arrow A). The euryhalinity of tilapia embryos seems to depend on the rapid and reversible changes between type-III cells and type-IV cells, as well as the continual presence of immature type-I cells, which can develop into the other cell types. Finally, we would like to emphasize that MRCs of euryhaline teleosts are not only important in understanding iono- and osmo-regulation of fishes, but also serve as a unique and excellent model for the ion transport properties of epithelial cells in general.

We thank Takeo Kurihara, Seikai National Fisheries Research Institute, for his advice on statistical analyses. Thanks are also due to Kaoru Funatsu, for her excellent

technical support for the triple-color immunostaining, and Kayoko Suenaga, Carl Zeiss Co., Ltd., for her technical guidance for confocal laser scanning microscopy. We are grateful to Norra Co., Ltd., for providing us 'Micros Ceramic', which was used as filter media for the brood-stock tanks.

References

Boisen, A. M., Amstrup, J., Novak, I. and Grosell, M. (2003). Sodium and chloride transport in soft water and hard water acclimated zebrafish (*Danio rerio*). *Biochim. Biophys. Acta* **1618**, 207-218.

Daborn, K., Cozzi, R. R. and Marshall, W. S. (2001). Dynamics of pavement cell-chloride cell interactions during abrupt salinity change in *Fundulus heteroclitus*. *J. Exp. Biol.* **204**, 1889-1899.

Evans, D. H., Piermarini, P. M. and Choe, K. P. (2005). The multifunctional fish gill: dominant site of gas exchange, osmoregulation, acid-base regulation, and excretion of nitrogenous waste. *Physiol. Rev.* **85**, 97-177.

Gagnon, E., Forbush, B., Caron, L. and Isenring, P. (2003). Functional comparison of renal Na-K-Cl cotransporters between distant species. *Am. J. Physiol. Cell Physiol.* **284**, C365-C370.

Goss, G., Perry, S. and Laurent, P. (1995). Ultrastructural and morphometric studies of ion and acid-base transport processes in freshwater fish. In *Fish Physiology*, vol. 14 (ed. C. M. Wood and T. J. Shuttleworth), pp. 257-284. San Diego, CA: Academic Press.

Haas, M. and Forbush, B., III (2000). The Na-K-Cl cotransporter of secretory epithelia. *Annu. Rev. Physiol.* **62**, 515-534.

Hiroi, J., Kaneko, T., Seikai, T. and Tanaka, M. (1998a). Developmental sequence of chloride cells in the body skin and gills of Japanese flounder (*Paralichthys olivaceus*) larvae. *Zool. Sci.* **15**, 455-460.

Hiroi, J., Kaneko, T., Uchida, K., Hasegawa, S. and Tanaka, M. (1998b). Immunolocalization of vacuolar-type H^+-ATPase in the yolk-sac membrane of tilapia (*Oreochromis mossambicus*) larvae. *Zool. Sci.* **15**, 447-453.

Hiroi, J., Kaneko, T. and Tanaka, M. (1999). *In vivo* sequential changes in chloride cell morphology in the yolk-sac membrane of Mozambique tilapia (*Oreochromis mossambicus*) embryos and larvae during seawater adaptation. *J. Exp. Biol.* **202**, 3485-3495.

Hwang, P. P. (1990). Salinity effects on development of chloride cells in the larvae of ayu (*Plecoglossus altivelis*). *Mar. Biol.* **107**, 1-7.

Hwang, P. P. and Hirano, R. (1985). Effects of environmental salinity on intercellular organization and junctional structure of chloride cells in early stages of teleost development. *J. Exp. Zool.* **236**, 115-126.

Kaneko, T., Shiraishi, K., Katoh, F., Hasegawa, S. and Hiroi, J. (2002). Chloride cells during early life stages of fish and their functional differentiation. *Fisheries Sci.* **68**, 1-9.

Kaplan, M. R., Plotkin, M. D., Lee, W. S., Xu, Z. C., Lytton, J. and Hebert, S. C. (1996). Apical localization of the Na-K-Cl cotransporter, *rBSC1*, on rat thick ascending limbs. *Kidney Int.* **49**, 40-47.

Katoh, F., Shimizu, A., Uchida, K. and Kaneko, T. (2000). Shift of chloride cell distribution during early life stages in seawater-adapted killifish, *Fundulus heteroclitus*. *Zoolog. Sci.* **17**, 11-18.

Katoh, F., Hyodo, S. and Kaneko, T. (2003). Vacuolar-type proton pump in the basolateral plasma membrane energizes ion uptake in branchial mitochondria-rich cells of killifish *Fundulus heteroclitus*, adapted to a low ion environment. *J. Exp. Biol.* **206**, 793-803.

Kirschner, L. B. (2004). The mechanism of sodium chloride uptake in hyperregulating aquatic animals. *J. Exp. Biol.* **207**, 1439-1452.

Lee, T. H., Hwang, P. P., Lin, H. C. and Huang, F. L. (1996). Mitochondria-rich cells in the branchial epithelium of the teleost, *Oreochromis mossambicus*, acclimated to various hypotonic environments. *Fish Physiol. Biochem.* **15**, 513-523.

Lin, L. Y. and Hwang, P. P. (2001). Modification of morphology and function of integument mitochondria-rich cells in tilapia larvae (*Oreochromis mossambicus*) acclimated to ambient chloride levels. *Physiol. Biochem. Zool.* **74**, 469-476.

Lin, L. Y. and Hwang, P. P. (2004). Mitochondria-rich cell activity in the yolk-sac membrane of tilapia (*Oreochromis mossambicus*) larvae acclimatized to different ambient chloride levels. *J. Exp. Biol.* **207**, 1335-1344.

Lytle, C., Xu, J. C., Biemesderfer, D. and Forbush, B., III (1995). Distribution and diversity of Na-K-Cl cotransport proteins: a study with monoclonal antibodies. *Am. J. Physiol.* **269**, C1496-C1505.

Marshall, W. S. (1995). Transport processes in isolated teleost epithelia: opercular epithelium and urinary bladder. In *Fish Physiology*, vol. 14 (ed. C. M. Wood and T. J. Shuttleworth), pp. 1-23. San Diego, CA: Academic Press.

Marshall, W. S. (2002). Na^+, Cl^-, Ca^{2+} and Zn^{2+} transport by fish gills: retrospective review and prospective synthesis. *J. Exp. Zool.* **293**, 264-283.

Marshall, W. S., Lynch, E. M. and Cozzi, R. R. (2002). Redistribution of immunofluorescence of CFTR anion channel and NKCC cotransporter in chloride cells during adaptation of the killifish *Fundulus heteroclitus* to sea water. *J. Exp. Biol.* **205**, 1265-1273.

McCormick, S. D., Sundell, K., Bjornsson, B. T., Brown, C. L. and Hiroi, J. (2003). Influence of salinity on the localization of Na^+/K^+-ATPase, $Na^+/K^+/2Cl^-$ cotransporter (NKCC) and CFTR anion channel in chloride cells of the Hawaiian goby (*Stenogobius hawaiiensis*). *J. Exp. Biol.* **206**, 4575-4583.

Nielsen, S., Maunsbach, A. B., Ecelbarger, C. A. and Knepper, M. A. (1998). Ultrastructural localization of Na-K-2Cl cotransporter in thick ascending limb and macula densa of rat kidney. *Am. J. Physiol.* **275**, F885-F893.

Onken, H., Tresguerres, M. and Luquet, C. M. (2003). Active NaCl absorption across posterior gills of hyperosmoregulating *Chasmagnathus granulatus*. *J. Exp. Biol.* **206**, 1017-1023.

Payne, J. A. and Forbush, B., III (1994). Alternatively spliced isoforms of the putative renal Na-K-Cl cotransporter are differentially distributed within the rabbit kidney. *Proc. Natl. Acad. Sci. USA* **91**, 4544-4548.

Pelis, R. M., Zydlewski, J. and McCormick, S. D. (2001). Gill Na^+-K^+-$2Cl^-$ cotransporter abundance and location in Atlantic salmon: effects of seawater and smolting. *Am. J. Physiol. Regul. Integr. Comp. Physiol.* **280**, R1844-R1852.

Perry, S. F., Shahsavarani, A., Georgalis, T., Bayaa, M., Furimsky, M. and Thomas, S. L. (2003). Channels, pumps, and exchangers in the gill and kidney of freshwater fishes: their role in ionic and acid-base regulation. *J. Exp. Zool. A. Comp. Exp. Biol.* **300**, 53-62.

Pisam, M. and Rambourg, A. (1991). Mitochondria-rich cells in the gill epithelium of teleost fishes: an ultrastructural approach. *Int. Rev. Cytol.* **130**, 191-232.

Riestenpatt, S., Onken, H. and Siebers, D. (1996). Active absorption of Na^+ and Cl^- across the gill epithelium of the shore crab *Carcinus maenas*: voltage-clamp and ion-flux studies. *J. Exp. Biol.* **199**, 1545-1554.

Sakamoto, T., Yokota, S. and Ando, M. (2000). Rapid morphological oscillation of mitochondrion-rich cell in estuarine mudskipper following salinity changes. *J. Exp. Zool.* **286**, 666-669.

Shiraishi, K., Kaneko, T., Hasegawa, S. and Hirano, T. (1997). Development of multicellular complexes of chloride cells in the yolk-sac membrane of tilapia (*Oreochromis mossambicus*) embryos and larvae in seawater. *Cell Tissue Res.* **288**, 583-590.

Silva, P., Solomon, R., Spokes, K. and Epstein, F. (1977). Ouabain inhibition of gill Na-K-ATPase: relationship to active chloride transport. *J. Exp. Zool.* **199**, 419-426.

Singer, T. D., Tucker, S. J., Marshall, W. S. and Higgins, C. F. (1998). A divergent CFTR homologue: highly regulated salt transport in the euryhaline teleost *F. heteroclitus*. *Am. J. Physiol.* **274**, C715-C723.

Suzuki, Y., Itakura, M., Kashiwagi, M., Nakamura, N., Matsuki, T., Sakuta, H., Naito, N., Takano, K., Fujita, T. and Hirose, S. (1999). Identification by differential display of a hypertonicity-inducible inward rectifier potassium channel highly expressed in chloride cells. *J. Biol. Chem.* **274**, 11376-11382.

Uchida, S. (2000). *In vivo* role of CLC chloride channels in the kidney. *Am. J. Physiol. Renal Physiol.* **279**, F802-F808.

Ura, K., Soyano, K., Omoto, N., Adachi, S. and Yamauchi, K. (1996). Localization of Na^+, K^+-ATPase in tissues of rabbit and teleosts using an antiserum directed against a partial sequence of the α-subunit. *Zoolog. Sci.* **13**, 219-227.

van der Heijden, A. J., van der Meij, J. C., Flik, G. and Wendelaar Bonga, S. E. (1999). Ultrastructure and distribution dynamics of chloride cells in tilapia larvae in fresh water and sea water. *Cell Tissue Res.* **297**, 119-130.

Wendelaar Bonga, S. E. and van der Meij, C. J. M. (1989). Degeneration and death, by apoptosis and necrosis, of the pavement and chloride cells in the gills of the teleost *Oreochromis mossambicus*. *Cell Tissue Res.* **255**, 235-243.

Wilson, J. M., Randall, D. J., Donowitz, M., Vogl, A. W. and Ip, A. K. (2000a). Immunolocalization of ion-transport proteins to branchial

epithelium mitochondria-rich cells in the mudskipper (*Periophthalmodon schlosseri*). *J. Exp. Biol.* **203**, 2297-2310.

Wilson, J. M., Laurent, P., Tufts, B. L., Benos, D. J., Donowitz, M., Vogl, A. W. and Randall, D. J. (2000b). NaCl uptake by the branchial epithelium in freshwater teleost fish: an immunological approach to ion-transport protein localization. *J. Exp. Biol.* **203**, 2279-2296.

Wu, Y. C., Lin, L. Y. and Lee, T. H. (2003). Na^+,K^+,$2Cl^-$cotransporter: a novel marker for identifying freshwater- and seawater-type mitochondria-rich cells in gills of the euryhaline tilapia, *Oreochromis mossambicus*. *Zool. Stud.* **42**, 186-192.

Xu, J. C., Lytle, C., Zhu, T. T., Payne, J. A., Benz, E., Jr and Forbush, B., III (1994). Molecular cloning and functional expression of the bumetanide-sensitive Na-K-Cl cotransporter. *Proc. Natl. Acad. Sci. USA* **91**, 2201-2205.

Xu, J. Z., Hall, A. E., Peterson, L. N., Bienkowski, M. J., Eessalu, T. E. and Hebert, S. C. (1997). Localization of the ROMK protein on apical membranes of rat kidney nephron segments. *Am. J. Physiol.* **273**, F739-F748.

Zar, J. H. (1999). *Biostatistical Analysis*, 4th edn. Upper Saddle River, NJ, USA: Prentice-Hall.